



## Transition metal-directed self-assembly of porphyrins bearing redox-active phenylenediamine pendant

Toru Amaya, Yasutomo Shimizu, Yasuhide Yakushi, Yumiko Nishina, Toshikazu Hirao\*

Department of Applied Chemistry, Graduate School of Engineering, Osaka University, Yamada-oka, Suita, Osaka 565-0871, Japan

### ARTICLE INFO

#### Article history:

Received 21 January 2010

Revised 16 February 2010

Accepted 22 February 2010

Available online 24 February 2010

#### Keywords:

Porphyrin

Oligoaniline

$\pi$ -Conjugated compound

Self-assembly

Au nanoparticles

### ABSTRACT

Synthesis and Zn(II)-directed self-assembly of the porphyrin–aniline trimer bearing the pyridyl group were demonstrated. Its Au nanoparticle hybrid was also synthesized.

© 2010 Elsevier Ltd. All rights reserved.

Controlled assembly of  $\pi$ -conjugated molecules can provide an organized redox-active nano-space.<sup>1</sup> Transition metal-directed assembly is regarded as a useful approach to architecturally controlled formation of conjugated polymeric complexes with  $\pi$ -conjugated ligands.<sup>2</sup> We have focused on the design, synthesis, and catalytic and material application of dimensionally controlled  $\pi$ -conjugated systems.<sup>3</sup> In the previous letters, aniline oligomers as redox-active  $\pi$ -conjugated ones were arranged on the porphyrin scaffold,<sup>4</sup> in which intramolecular photo-induced electron transfer is performed from the phenylenediamine moiety to the porphyrin. We also demonstrated the sandwich-type assembly of the zinc complexes of such molecules by coordination of bidentate ligands.<sup>5</sup> Introduction of a metal coordination site into such molecules is considered to allow the metal ion-directed self-assembly. Due to the existence of a vacant axial coordination site in a five-coordinated metal ion/porphyrin complex, such as a Zn(II) one, polymeric, and/or oligomeric nanowire structures are considered to be formed through intermolecular self-assembly (Fig. 1). The assembly on the metal nanoparticle surface is also expected. According to this concept, oligoaniline–porphyrin hybrids **1** and **2** were designed, where a pyridine moiety as a metal coordination site was incorporated into the terminal of the oligoaniline chain. Here, we report the synthesis and Zn(II)-directed self-assembly of porphyrin–aniline trimer hybrids **1** and **2** (Scheme 1). The assembly of **1** on Au nanoparticles is also described.

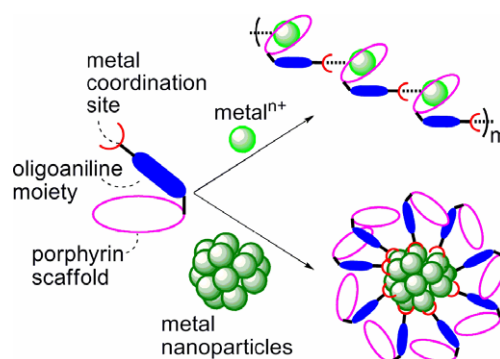
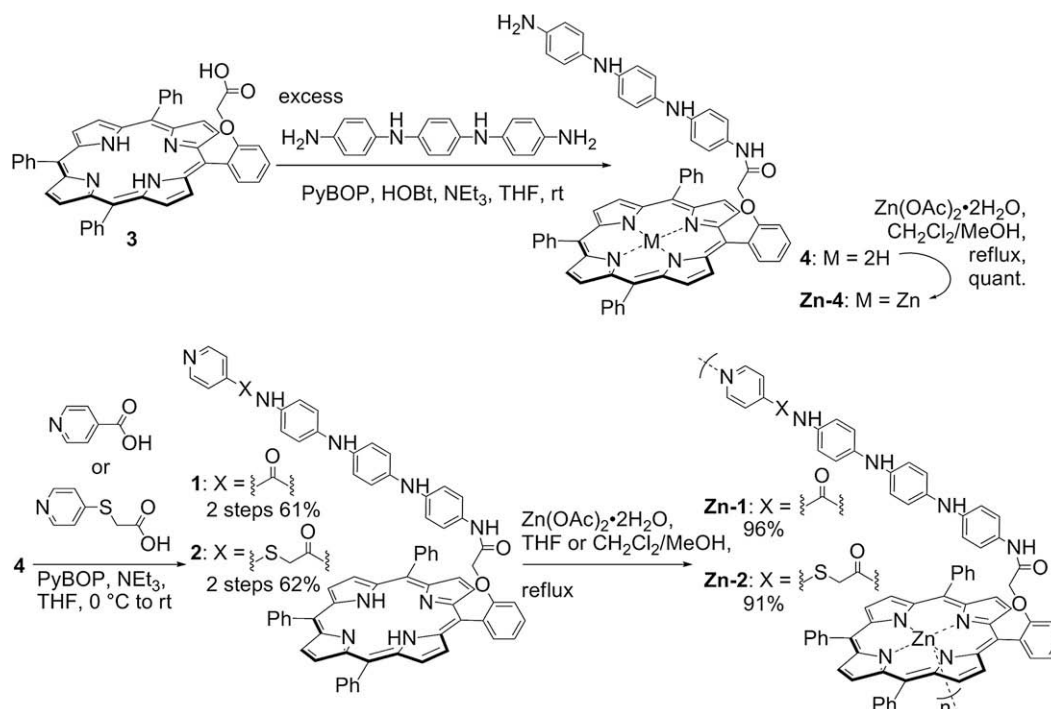


**Figure 1.** Schematic representation of transition metal-directed self-assembly of porphyrins bearing an oligoaniline moiety with a metal coordination site.

Scheme 1 shows the synthesis of **1**, **2**, and their Zn(II) complexes **Zn-1** and **Zn-2**. Carboxylic acid **3** and  $N^1,N^{1'}$ -(1,4-phenylene)dibenzene-1,4-diamine were prepared according to the reported procedures.<sup>6,7</sup> In the presence of an excess amount of the diamine, condensation reaction of **3** with the diamine using PyBOP gave the coupling product **4**. The obtained porphyrin **4** was coupled with isonicotinic acid or 2-(pyridin-4-ylthio)acetic acid to afford the amide **1** or **2** (two-step yield, 61% and 62%, respectively). The model aniline chains **5** and **6** without the porphyrin moiety were also prepared (see Supplementary data). 4-Pyridylthio group has a higher basicity than the pyridyl group of the isonicotinic acid moiety. Therefore, the former is expected to show a greater affinity

\* Corresponding author. Tel.: +81 6 6879 7413; fax: +81 6 6879 7415.  
E-mail address: [hirao@chem.eng.osaka-u.ac.jp](mailto:hirao@chem.eng.osaka-u.ac.jp) (T. Hirao).



**Scheme 1.** Synthesis of **1**, **2**, and their Zn(II) complexes **Zn-1** and **Zn-2**.

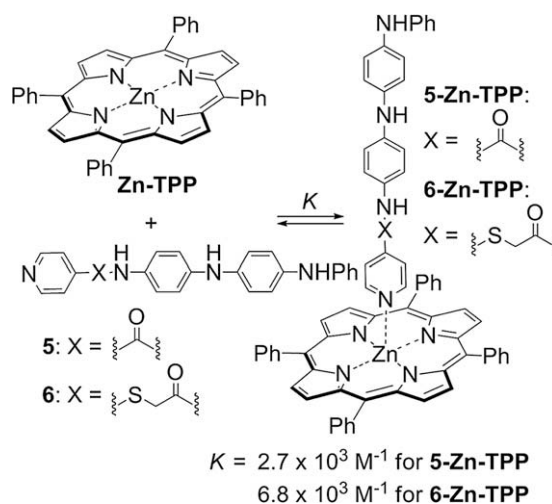
**Table 1**

Chemical shifts of **1**, **2**, **Zn-1**, **Zn-2**, and **7** (DMSO-*d*<sub>6</sub>, 600 MHz)

	$\text{R}^1\text{-O-CO-NH}^1$	$\text{H}^1$	$\text{H}^2$	$\text{H}^3$	$\text{H}^4$	$\text{R}^2$	<b>7: R<sup>1</sup> = Ph, R<sup>2</sup> = C<sub>5</sub>H<sub>5</sub>N</b>					
	$-\text{OCH}_2\text{CO}-$	$-\text{NH}^1-$	a ( $\Delta\delta$ )	b ( $\Delta\delta$ )	$-\text{NH}^2-$	c	d	$-\text{NH}^3-$	e	f	$-\text{NH}^4-$	
<b>1</b>	4.55	7.30	5.55 (1.89)	5.87 (1.06)	7.46	6.67	6.95	7.89	6.98	7.60	10.33	
<b>2</b>	4.55	7.24	5.51 (1.93)	5.83 (1.10)	7.40	6.63	6.90	7.79	6.92	7.40	10.10	
<b>Zn-1</b>	4.56	6.89	5.36 (2.08)	5.85 (1.08)	7.43	6.65	6.93	7.87	6.97	7.60	10.32	
<b>Zn-2</b>	4.56	6.87	5.34 (2.10)	5.82 (1.11)	7.41	6.62	6.89	7.80	6.92	7.40	10.12	
<b>7</b>	4.63	9.84	7.44	6.93	7.81	6.99	6.99	7.86	6.96	7.56	10.29	

toward Zn(II)-porphyrins than the latter. Treatment of **1** and **2** with Zn(OAc)<sub>2</sub>·2H<sub>2</sub>O gave the self-assembled products **Zn-1** and **Zn-2** in 96% and 91% yields, respectively. Conformation of **1**, **2**, **Zn-1**, and **Zn-2** in a DMSO-*d*<sub>6</sub> solution was investigated by <sup>1</sup>H NMR. DMSO-*d*<sub>6</sub> inhibits the coordination of the pyridyl group to **Zn-1** and **Zn-2**, which are probably present in a monomeric state. Table 1 shows the selected chemical shifts for the aniline chains. The protons close to the porphyrin ring exhibited the remarkable higher field shift in all compounds. The  $\Delta\delta$ , which is the difference in the chemical shift from the model aniline chain **7**, reached approximately 2 and 1 ppm at the protons a and b, respectively (Table 1). These shifts are explained by the ring-current effect of the porphyrin  $\pi$ -system. This suggests that the aniline chain leans toward the porphyrin ring.

To estimate the binding constant of the pyridyl group to the Zn(II)-porphyrin, the titration experiment was conducted using the model compounds **5** and **6** (Scheme 2). The CH<sub>2</sub>Cl<sub>2</sub> solution of **5** or **6** was added to the CH<sub>2</sub>Cl<sub>2</sub> solution of Zn(II)-tetraphenyl porphyrin (**Zn-TPP**), and the complexation behavior was tracked by UV-vis absorption spectroscopy (Figs. S1 and S2). The peaks of the Soret and Q bands red-shifted as the coordination of the pyridyl group progressed. The binding constants *K* for **5** and **6** were calculated to be  $2.7 \times 10^3$  and  $6.8 \times 10^3$  M<sup>-1</sup>, respectively. As expected, the latter exhibited the larger value.



**Scheme 2.** Equilibrium for the coordination of oligoaniline **5** or **6** toward **Zn-TPP** to form the complex **5-Zn-TPP** or **6-Zn-TPP**.

Electronic environment of **1**, **2**, **4**, **TPP**, and their Zn(II) complexes **Zn-1**, **Zn-2**, **Zn-4**, and **Zn-TPP** was investigated by UV-vis

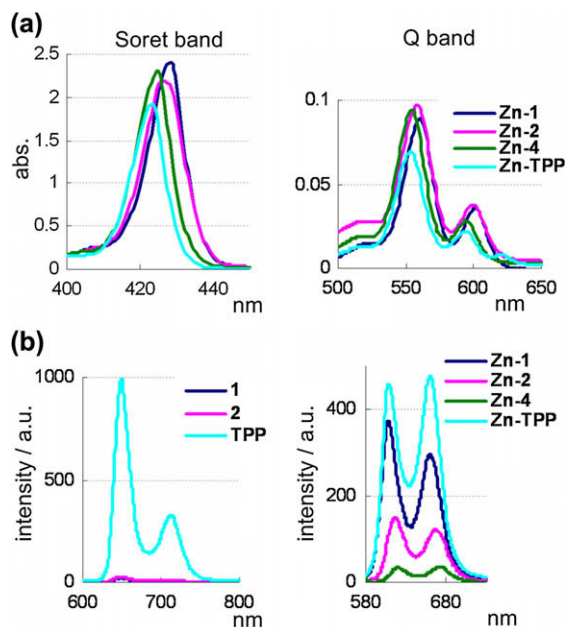


**Figure 2.** (a) UV-vis absorption spectra of Soret and Q band region for **Zn-1**, **Zn-2**, **Zn-4**, and **Zn-TPP**. (b) Emission spectra of **1**, **2**, **TPP**, **Zn-1**, **Zn-2**, **Zn-4**, and **Zn-TPP** with excitation of the  $Q_y(1,0)$  or  $Q(1,0)$  band for the free base porphyrins or Zn-porphyrins, respectively.  $5.0 \times 10^{-6}$  M solution of  $\text{CH}_2\text{Cl}_2/\text{THF} = 995:5$  under argon atmosphere.

absorption spectroscopy. Measurement was carried out in the  $5.0 \times 10^{-6}$  M solution of  $\text{CH}_2\text{Cl}_2/\text{THF} = 995:5$  under argon atmosphere.<sup>8</sup> Porphyrins bearing an aniline chain showed a broad absorption around 280–350 nm derived from the aniline chain as well as the characteristic Soret and Q bands (Fig. S3). Red-shift of Soret and Q bands was observed with the Zn complex, **Zn-1** and **Zn-2**, as compared with **Zn-TPP**, however, the smaller shift was observed with the **Zn-4** complex which does not have a pyridyl moiety (Figs. 2a and S4). The coordination of the pyridyl group to the Zn-porphyrin is likely to contribute to the red-shift. Thus, the self-assembly of the porphyrin bearing an aniline chain was suggested.

Fluorescence emission spectroscopy with excitation of the  $Q_y(1,0)$  or  $Q(1,0)$  band was studied with **1**, **2**, **TPP**, and their Zn(II) complexes, **Zn-1**, **Zn-2**, **Zn-4**, and **Zn-TPP** (Fig. 2b).<sup>9</sup> Measurement was also carried out in the  $5.0 \times 10^{-6}$  M solution of  $\text{CH}_2\text{Cl}_2/\text{THF} = 995:5$  under argon atmosphere. Significant quenching was observed with **1** and **2** bearing the aniline chain, as compared with that of **TPP**. It is likely due to the intramolecular photo-induced electron transfer. This phenomenon was also consistent with our previous reports.<sup>4</sup> When the model aniline chain was added to

**Table 2**

The redox potential (V vs  $F_c/F_c^+$ ) and driving force of the photo-induced charge separation  $\Delta G_{CS}$  (V) for **1**, **2**, **TPP**, **Zn-1**, **Zn-2**, **Zn-TPP**, and **7** (0.25 mM in THF containing 0.1 M  $\text{Bu}_4\text{NClO}_4$ )

	Redox potential (V vs $F_c/F_c^+$ )		$\Delta G_{CS}^a$ (V)
	$E(\text{Por}/\text{Por}^-)$	$E(D^+/D)$	
<b>1</b>	-1.68	-0.14	-0.38
<b>2</b>	-1.68	-0.14	-0.38
<b>TPP</b>	-1.70	+0.60	—
<b>Zn-1</b>	-1.93	-0.14	-0.26
<b>Zn-2</b>	-1.90	-0.15	-0.29
<b>Zn-TPP</b>	-1.93	+0.40	—
<b>7</b>	—	-0.14	—

<sup>a</sup>  $E(D^+/D) - E(A/A^-) - E_{00}$ , where  $E_{00}$  is the energy of photoexcitation.

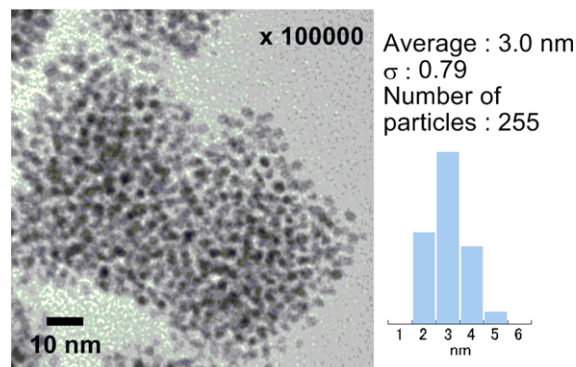
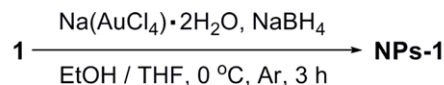


**Figure 3.** Synthesis of **NPs-1** and its TEM image.

the solution of **TPP**, the decreasing of emission intensity was observed with the increasing of the concentration of the aniline chain. Stern–Volmer plot gave a linear relationship, and the Stern–Volmer constant was  $1.6 \times 10^3 \text{ M}^{-1}$  (Fig. S5). Concerning about the Zn(II)-complexes **Zn-1**, **Zn-2**, and **Zn-4** bearing the aniline chain, their emission intensity was also smaller than that of **Zn-TPP**. **Zn-1** and **Zn-2** showed the larger emission than **Zn-4**, where the coordination from the pyridyl moiety to the Zn(II) center is likely to contribute.

First oxidation and reduction potentials were obtained from the differential pulse voltammograms of **1**, **2**, **7**, **TPP**, and their Zn complexes **Zn-1**, **Zn-2**, and **Zn-TPP** (Fig. S6). Measurement was carried out in their 0.25 mM THF solution with  $\text{Bu}_4\text{NClO}_4$  as an electrolyte under argon atmosphere. Table 2 shows the potentials versus  $F_c/F_c^+$  and the driving force of photo-induced charge separation  $\Delta G_{CS}$  estimated by the equation:  $\Delta G_{CS} = E(D^+/D) - E(A/A^-) - E_{00}$ , where  $E_{00}$  is the energy of photoexcitation. First oxidation potentials are approximately -0.14 V for **1**, **2**, **Zn-1**, **Zn-2**, and **7**, assigned to the one-electron oxidation of the aniline chain. On the other hand, first reduction potentials are approximately -1.7 V for free base porphyrins **1**, **2**, and **TPP**, and -1.9 V for Zn(II)-complexes **Zn-1**, **Zn-2**, and **Zn-TPP**. Negative  $\Delta G_{CS}$  was observed with **1**, **2**, **Zn-1**, and **Zn-2**, which supports the results of decreasing of the emission and suggests the intramolecular electron transfer.

Pyridyl group is known to act as a protecting group for Au nanoparticles.<sup>10</sup> So, Au nanoparticles **NPs-1** were synthesized by the reduction of  $\text{Na(AuCl}_4)$  using  $\text{NaBH}_4$  in the presence of the porphyrin **1**. Its transmission electron microscopy (TEM) image is shown in Figure 3. The average diameter is 3.0 nm and the particles are independent.  $^1\text{H}$  NMR showed the presence of the porphyrins without decomposition. There is no doubt that the porphyrins act as a protecting group for the Au nanoparticles although direct evidence was not obtained for the coordination of the pyridyl group to the Au nanoparticles.

In summary, synthesis and Zn(II)-induced self-assembly of **1** and **2** were demonstrated. Au nanoparticles protected with **1** were also synthesized. They are of potential use in a variety of applications such as redox-active receptors and photo-active catalysts or materials. Further investigation is now in progress.

#### Acknowledgments

The authors thank Ms. Toshiko Muneishi at Osaka University for the measurement of the NMR spectra. This work was partially supported by a Grant-in-Aid for Scientific Research on Priority Areas

“Chemistry of Concerto Catalysis” from the Ministry of Education, Culture, Sports, Science, and Technology, Japan.

### Supplementary data

Supplementary data associated with this article can be found, in the online version, at doi:10.1016/j.tetlet.2010.02.120.

### References and notes

1. *Redox Systems Under Nano-Space Control*; Hirao, T., Ed.; Springer: Berlin, Heidelberg, New York, 2006.
2. (a) Fujita, M.; Umemoto, K.; Yoshizawa, M.; Fujita, N.; Kusukawa, T.; Biradha, K. *Chem. Commun.* **2001**, 509; (b) Holliday, B. J.; Mirkin, C. A. *Angew. Chem., Int. Ed.* **2001**, 40, 2022; (c) Kobuke, Y.; Ogawa, K. *Bull. Chem. Soc. Jpn.* **2003**, 76, 689; (d) Ruben, M.; Rojo, J.; Romero-Salguero, F. J.; Uppadine, L. H.; Lehn, J.-M. *Angew. Chem., Int. Ed.* **2004**, 43, 3644.
3. For an account, see: (a) Hirao, T. *Coord. Chem. Rev.* **2002**, 226, 81. and references cited therein; (b) Hirao, T.; Iida, K. *Chem. Commun.* **2001**, 431; (c) Saito, K.; Hirao, T. *Bull. Chem. Soc. Jpn.* **2002**, 75, 1845.
4. (a) Hirao, T.; Saito, K. *Tetrahedron Lett.* **2000**, 41, 1413; (b) Saito, K.; Hirao, T. *Tetrahedron* **2002**, 58, 7491; (c) Hirao, T.; Saito, K. *Macromol. Symp.* **2003**, 204, 103; (d) Amaya, T.; Mori, K.; Hirao, T. *Heterocycles* **2009**, 78, 2729.
5. Hirao, T.; Saito, K. *Synlett* **2002**, 415.
6. Verboom, R. C.; Slagt, V. F.; Bäckvall, J.-E. *Chem. Commun.* **2005**, 1282.
7. Różalska, I.; Kulyk, P.; Kulszewicz-Bajer, I. *New J. Chem.* **2004**, 28, 1235.
8. 0.5% THF co-solvent was used due to the solubility of the compounds, where the complexation was ligand exchange with THF.
9. Excitation at 515, 515, 514, 561, 558, 555, and 554 nm for **1**, **2**, **TPP**, **Zn-1**, **Zn-2**, **Zn-4**, and **Zn-TPP**, respectively.
10. Gittins, D. I.; Caruso, F. *Angew. Chem., Int. Ed.* **2001**, 40, 3001.